Drug Design, Development and Therapy

Dovepress

open access to scientific and medical research

Open Access Full Text Article

ORIGINAL RESEARCH

Shikonin Could Be Used to Treat Tubal Pregnancy via Enhancing Ferroptosis Sensitivity

Yuling Lai[1,2], Fuling Zeng[1], Zhenyue Chen[1], Min Feng[1], Yanxi Huang[3], Pin Qiu[3], Lihua Zeng[1], Yan Ke[4], Gaopi Deng[3,*], Jie Gao[3,*]

[1]First Clinical Medical College, Guangzhou University of Chinese Medicine, Guangzhou, People's Republic of China; [2]Department of Sports Medicine, Guangzhou Sport University, Guangzhou, People's Republic of China; [3]Department of Gynaecology, The First Affiliated Hospital of Guangzhou University of Chinese Medicine, Guangzhou, People's Republic of China; [4]Department of Gynaecology, Shenzhen Chinese and Western Medicine Hospital, Shenzhen, People's Republic of China

*These authors contributed equally to this work

Correspondence: Jie Gao; Gaopi Deng, Email gaojie1769@gzucm.edu.cn; denggaopi@126.com

Background: Albeit oxidative stress has been implied in the pathogenesis of tubal pregnancy (TP), there are scant data to suggest that ferroptosis occurs in TP. Shikonin plays a pivotal role in redox status, but whether it can regulate ferroptosis to treat TP remains unknown.

Methods: We collected and analyzed ferroptosis-related indices from the villous tissue (VT) of women suffering from TP and from women with a normal pregnancy. In vitro, we used shikonin and/or RAS-selective lethal 3 (RSL3) to intervene HTR-8/SVneo cells and further detected ferroptosis indices and cell functions. Finally, the expression of the nuclear factor erythroid 2-related factor 2 (Nrf2) is pharmacologically activated to explore the effect of Nrf2 on shikonin regulating ferroptosis.

Results: Increased malondialdehyde content, reduced levels of glutathione and glutathione peroxidase (GPx), and upregulated protein expression which promoted ferroptosis were observed in the VT of TP patients, suggesting that ferroptosis occurred during TP. In vitro, shikonin enhanced ferroptosis sensitivity in HTR-8/SVneo cells induced by RSL3 via amplifying lipid peroxidation, which mainly included increasing cellular reactive oxygen species (ROS), lipid ROS and Fe^{2+} level. RSL3 and/or shikonin inhibited Nrf2 and downregulated protein expression of SLC7A11 and GPx4 caused by RSL3 + shikonin co-treatment, which could be reversed under activation of Nrf2. Hence, shikonin facilitated lipid peroxidation by inhibiting Nrf2 signaling. Additionally, shikonin and/or RSL3 potently inhibited the invasion and migration of HTR-8/SVneo cells.

Conclusion: This study firstly showed that ferroptosis may be involved in TP pathogenesis and shikonin potentially targeted ferroptosis to treat TP.

Keywords: ectopic pregnancy, shikonin, lipid peroxidation, iron dependent

Introduction

"Tubal pregnancy" (TP) refers to the implantation and development of a fertilized ovum in a fallopian tube. TP is a main reproductive health issue for women and accounts for 1–2% of all pregnancies.[1] Despite its prevalence, the underlying pathogenesis of TP is poorly understood.[2] An imbalance between oxidant and antioxidant processes may alter the tubal environment and reduce tubal ciliary pulsation and smooth-muscle contractions which, in turn, increase the risk of TP by disrupting transport mechanisms in the embryo.[3] However, few studies have focused on lipid peroxidation in TP.

Ferroptosis is a recently identified form of programmed cell death. Distinct from other forms of regulated cell death (eg, apoptosis, autophagy), ferroptosis is characterized by accumulation of iron-dependent lipid peroxidation to a lethal level.[4] Ferroptosis is reliant upon reactive oxygen species (ROS), phospholipids containing polyunsaturated fatty acids (PUFAs), and iron.[5] Recent studies have demonstrated the role of ferroptosis in trophoblastic injury and placental dysfunction (which mainly involves lipid peroxidation in embryo injury) and iron-dependent lipid peroxidation is abundant in trophoblasts.[4]

Received: 7 March 2022
Accepted: 14 June 2022
Published: 1 July 2022

According to a study based on next-generation sequencing of RNA from placental cells, ferroptosis-related genes (ferroportin, iron-responsive element-binding protein-2, ferritin heavy chain-1 (FTH1)) show high expression in cytotrophoblasts, syncytiotrophoblasts and decidua cells, which suggests that different cell lines on the maternal–fetal interface are vulnerable to iron regulation.[6] In addition, lysophosphatidylcholine acyltransferase 3 (LPCAT3)[6] and acyl-coA synthetase long-chain family member 4 (ACSL4),[7–9] which are crucial in the biosynthesis and remodeling of PUFA-phosphatidylethanolamine phospholipids, have high expression in trophoblasts and provide abundant PUFA substrate for ferroptosis. A hypoxic environment is more obvious in TP because the fallopian tubes fail to build a complete decidua. The mitochondrial electron transport chain is impaired under a hypoxic environment, and further produces mounts of ROS to trigger ferroptosis. Therefore, this research hypothesized that ferroptosis may contribute to the occurrence and development of TP.

Shikonin is a naphthoquinone compound extracted from the root of *Lithospermum erythrorhizon*. Studies have shown that ROS generation and glutathione (GSH) depletion resulting from shikonin treatment trigger disruption of the mitochondrial transmembrane potential.[10] Since the inhibition of GSH synthesis and the increase of ROS were considered as key events of ferroptosis, whether the dominant effect of shikonin on regulating GSH and ROS could promote ferroptosis arouses the interest. Combined treatment of shikonin with 2-2-Deoxy-d-glucose has been shown to suppress the glycolytic phenotype through modulation of the reduced nicotinamide adenine dinucleotide phosphate (NADPH) oxidase 4/protein kinase B signaling pathway in glioblastomas.[11] Shikonin treatment can target the Sec residue in thioredoxin reductase 1 (TrxR1) to inhibit its physiological function, but changes the enzyme to an NADPH oxidase to generate superoxide anions, which leads to ROS production and collapse of the intracellular redox balance.[12] NAPDH is an essential cofactor and electron donor that supplements GSH content and maintains the redox balance. NAPDH quinone oxidoreductase-1 (NQO1) is involved in two-electron reduction. NQO1 can transform certain quinone compounds into cytotoxic agents, thereby resulting in cell death.[13] NQO1 is regulated by the antioxidant responsive element (ARE), which is mainly activated by nuclear factor erythroid 2-related factor 2 (Nrf2).[14] As a core transcription factor in the oxidative pathway, Nrf2 has downstream targets which have been postulated to inhibit ferroptosis, such as solute carrier family 7 member 11 (SLC7A11) and glutathione peroxidase 4 (GPx4).[15] The major sources of intracellular ROS involve NAPDH oxidase, xanthine/xanthine oxidase, lipoxygenase and the mitochondrial respiratory chain.[16] Lipid peroxidation driven by excessive ROS is a basic feature of ferroptosis, and the relationship between Nrf2 and ferroptosis has been demonstrated. Hence, we hypothesized that shikonin exposure might induce or enhance ferroptosis via Nrf2 signaling.

The link between ferroptosis and TP pathogenesis has not been reported. In the present study, we found that key proteins involved in ferroptosis regulation had abnormal expression in the villous tissue (VT) of TP patients, and that lipid oxidation was activated markedly. In vitro experiments revealed that shikonin promoted RAS-selective lethal 3 (RSL3)-induced ferroptosis and inhibited the invasion and migration abilities of trophoblasts. The potential mechanism of ferroptosis in TP was discussed. This study will help to further clarify the pathogenesis and improve the treatment of TP.

Materials and Methods

Ethics Statement

The study protocol was approved (K [2019]136) by the Research Medical Ethics Committee of The First Affiliated Hospital of Guangzhou University of Chinese Medicine (Guangzhou, China). Patients and healthy volunteers provided written informed consent before they participated in this study. The study was conducted in accordance with the Declaration of Helsinki 1964 and its later amendments.

Inclusion and Exclusion Criteria

All patients in each group had no primary diseases such as hypertension, diabetes mellitus, hypo-hyperthyroidism, renal or liver failure; no history of drug treatment in recent 3 months; or no smokers and/or alcohol abusers were included in the study.

The TP group involved in patients who were diagnosed with TP by elevated β- hCG and by TVUS (Transvaginal Ultrasound) image which indicated the possible gestational sac located in fallopian tubes. Pathological examination was performed for the excretion or scraping of the uterine cavity and no villous tissue was found in the section. Patients with

ectopic pregnancies located outside the fallopian tubes with hemodynamic instability at admission were excluded from the study.

The control (pregnancy) group involved women in the first trimester and were confirmed as normal intrauterine pregnancy by TVUS. Pathological examination was performed for the excretion or scraping of the uterine cavity and villous tissue could be found in the section.

Study Cohort

The study population comprised TP patients (n = 15) and women with a physiologically normal pregnancy (n = 15). The clinical data of participants is presented in Table 1. Human VT was collected from First Affiliated Hospital of Guangzhou University of Chinese medicine. A portion of VT was stored at −80°C for measurement of protein expression. The other portion of VT was fixed with 4% paraformaldehyde (PFA) and embedded in paraffin.

Table 1 Medical Record Information

Patient Number	Age (Years)	Gestational Weeks	Pregnancy and Delivery History
NP1	27	6+	G1P0A0
NP2	22	7+	G1P0A0
NP3	23	6+	G2P0A1
NP4	22	6+	G2P0A1
NP5	22	7+	G1P0A0
NP6	24	7+	G1P0A0
NP7	22	6+	G1P0A0
NP8	29	7+	G1P0A0
NP9	25	7+	G1P0A0
NP10	22	7+	G1P0A0
NP11	24	6+	G1P0A0
NP12	24	7+	G2P0A1
NP13	22	6	G1P0A0
NP14	24	7+	G1P0A0
NP15	23	6+	G1P0A0
TP1	35	7+	G2P1A0
TP2	30	6+	G2P0A1
TP3	21	7+	G3P0A2
TP4	29	5+	G3P2A0
TP5	28	7+	G1P0A0
TP6	23	7+	G2P1A0
TP7	30	7	G2P1A0
TP8	31	6+	G1P0A1

(*Continued*)

Table 1 (Continued).

Patient Number	Age (Years)	Gestational Weeks	Pregnancy and Delivery History
TP9	32	6+	G3P1A1
TP10	33	8	G2P1A0
TP11	21	6	G3P1A1
TP12	21	6+	G2P0EP1
TP13	35	5	G3P1A1
TP14	25	6+	G2P1A1
TP15	35	6+	G3P1EP1

Culture and Treatment of HTR-8/SVneo Cells

The HTR-8/SVneo cell line is generated using freshly isolated syncytiotrophoblasts from first-trimester placentas.[17] This cell line is employed to study the invasion and proliferation of trophoblasts.[18] HTR-8/SVneo cells were obtained from the American Type Culture Collection (Manassas, VT, USA) and maintained in RPMI-1640 medium (Gibco, Grand Island, NY, USA) supplemented with 10% fetal bovine serum (Gibco) and antibiotics (penicillin 100 IU/mL and streptomycin 100 μg/mL) in a humidified atmosphere of 5% CO_2 at 37°C. Inhibitors of ferroptosis (ferrostatin-1 (Fer-1; 0.1 μM), deferoxamine (DFO; 10 μm) or inhibitors of autophagy (chloroquine (CQ; 5 μM)) were added to cells cultured under the RSL3 + shikonin condition to determine the cell death induced by RSL3 + shikonin.

Chemicals and Reagents

Erastin (catalog number: S7242), RSL3 (S8155), Fer-1 (S7243) and DFO (S5742) were from Selleck Chemicals (Houston, TX, USA). Shikonin (110769-200405) was purchased from the National Institutes for Food and Drug Control. Chloroquine (C6628) was obtained from MilliporeSigma (Burlington, MA, USA). Tertiary butylhydroquinone (t-BHQ; IT1150) was sourced from Solarbio (Beijing, China). Primary and secondary antibodies used for Western blotting, immunohistochemistry or immunofluorescence staining are listed in Supplementary Table S1.

Measurement of GSH Content and GPx Activity

VT and cell samples were lysed with radioimmunoprecipitation (RIPA) lysis buffer (P0013B; Beyotime Institute of Biotechnology, Shanghai, China). The cellular level of GSH was measured using a GSH Assay Kit, according to manufacturer (Beyotime Institute of Biotechnology) instructions. GPx activity was tested using a Glutathione Peroxidase Assay kit with NADPH (S0056; Beyotime Institute of Biotechnology) following manufacturer's instructions.

Measurement of Malondialdehyde (MDA) Level

Membrane lipid peroxidation was determined using a Lipid Peroxidation MDA Assay Kit (S0131S; Beyotime Institute of Biotechnology). VT and cell samples were lysed, and the supernatant (100 μL) was mixed with MDA working solution in a 1.5-mL centrifugal tube. Subsequently, the tube was heated to 100°C for 15 min, followed by thawing on ice. The solution was centrifuged at 1000 × g for 10 min at room temperature, and then the optical density of the supernatant was determined at 532 nm.

Western Blotting

VT and cells were lysed on ice for 30 min using RIPA lysis buffer. Lysates were heated for 5 min at 100°C. Then, equal amounts of lysates were subjected to sodium dodecyl sulfate–polyacrylamide gel electrophoresis and transferred onto polyvinylidene difluoride (PVDF) membranes. PVDF membranes were blocked with 5% non-fat milk for 2 h at room

temperature and incubated overnight at 4°C with primary antibodies against GPx4, SLC7A11, ACSL4, transferrin receptor-1 (TfR1), microtubule-associated protein 1 light chain 3B (LC3B), P62, Nrf2, NQO1, glyceraldehyde-3-phosphate dehydrogenase (GAPDH) and β-actin. PVDF membranes were incubated with horseradish peroxidase-conjugated anti-rabbit immunoglobulin (Ig)G for 1 h. Target bands were detected using electrochemiluminescence reagent in a multifunctional imager (Bio-Rad Laboratories, Hercules, CA, USA) and densitometric analysis was done using ImageJ (National Institutes of Health, Bethesda, MD, USA).

Perls' Staining

VT collected from Guangzhou University of Chinese Medicine was fixed with 4% PFA for 24 h. Samples were embedded in paraffin and cut into sections of thickness 4 μm. Then, the paraffin sections were dewaxed and hydrated. Next, non-haem iron staining was done using standard Perls' blue solution (Bestbio, Beijing, China). Images were captured with a light microscope (Olympus, Tokyo, Japan).

Immunohistochemical (IHC) and Immunofluorescence (IF) Staining

Heat-induced antigen retrieval was undertaken using EDTA antigen retrieval solution (Beyotime Institute of Biotechnology) after paraffin sections had been dewaxed and hydrated.

For IHC staining, sections were pretreated with Endogenous Peroxidase Blocking Buffer (ZSGB-Bio, Beijing, China) for 10 min for antigen retrieval. Then, sections were incubated with primary antibodies against GPx4, SLC7A11, ACSL4, TfR1 and Nrf2 overnight at 4°C. A horseradish peroxidase-conjugated compact polymer system was employed.

For IF staining, after high-temperature and high-pressure repairments, sections were washed with phosphate-buffered saline (PBS) and blocked with 5% bovine serum albumin. Then, sections were incubated with anti-Nrf2 antibody overnight at 4°C (for immunofluorescence of cells, primary antibodies against GPx4, ACSL4 and Nrf2 were used). Fluorescein isothiocyanate-conjugated anti-rabbit IgG was applied appropriately, and the nuclei were stained with 4′,6-diamidino-2-phenylindole. Images were captured under a microscope (Olympus).

Cell Viability Assay

Cell viability was evaluated using Cell Counting Kit-8 (CCK8) (Dojindo, Japan) assay, according to manufacturer's instructions. $10\times^{4}$ cells per well were seeded in 96-well plates. CCK8 regent was added and incubated for 2 h at 37°C. The optical absorbance was measured at 450 nm using a microplate reader (Thermo Fisher Scientific, America).

Wound-Healing Assay

HTR-8/SVneo cells (4×10^5) were seeded into six-well plates and grown to >90% confluence. Then, cell monolayers were scraped using a pipette tip to create wounds. After treatment as indicated, cells were rinsed twice with fresh RPMI-1640 medium and culture permitted for an additional 24 h. Images were captured at 0 h and 24 h under a microscope (Olympus) and analyzed by ImageJ.

Cell Invasion Assay

Cells (1×10^5) were seeded onto the upper chambers of a Transwell™ membrane (Corning, Corning. NY, USA) with serum-free RPMI-1640 medium that had been precoated with Matrigel™ (Corning) 4 h before cell seeding. The lower chambers were filled with RPMI-1640 medium containing 20% fetal bovine serum. After treatment as indicated, cells attached to the reverse side of the membrane were fixed with 4% PFA and stained with crystal violet. Images were photographed under a microscope (Olympus) and analyzed by ImageJ.

ROS Detection

2′,7′-Dichlorofluorescin diacetate (DCFH-DA) Probe

The intracellular level of ROS was evaluated using a 2′,7′-Dichlorofluorescin diacetate (DCFH-DA) fluorescent probe (Beyotime Institute of Biotechnology). HTR-8/SVneo cells were seeded in six-well plates (1×10^5 cells/well) and treated

under the designated conditions. After treatment as indicated, cells were incubated with DCFH-DA (10 μM/L) for 20 min in the dark and then washed thrice with PBS. Images were captured using a fluorescence microscope (Olympus).

C11-BODIPY$^{581/591}$ Probe

In general, C11-BODIPY$^{581/591}$ is used to monitor the flux of lipid ROS in cell membranes. The level of lipid ROS was evaluated via a C11-BODIPY fluorescent probe (ABclonal, Woburn, MA, USA). HTR-8/SVneo cells were seeded in six-well plates (1×10^4 cells/well) and treated under the designated conditions. After treatment as indicated, the probe (50 μM) was added and the solution was allowed to incubate for 1 h in the dark and then washed thrice with PBS. Lasers set at 488 nm and 565 nm were used to excite the solution. Fluorescence images were collected under a confocal laser scanning microscope (Leica, Wetzlar, Germany).

Labile Iron Pool (LIP) Assay

"Labile iron" (which is primarily in the ferrous (Fe^{2+}) form) is a small, transitional pool of intracellular iron, and commonly termed "LIP". LIP release was measured using a FeRhoNox-1™ (Fe^{2+} indicator) fluorescent probe (MKBio, Beijing, China). HTR-8/SVneo cells were plated in six-well plates, loaded with FeRhoNox-1 (5 μM) for 30 min at 37°C and then washed thrice with Hanks' balanced salt solution. Cells were observed under a fluorescence microscope (Olympus).

Mitochondrial Morphology

MitoTracker™ Green (Beyotime Institute of Biotechnology) was used for labeling of the mitochondria of living cells using fluorescence. RPMI-1640 medium was removed, and then MitoTracker Green (100 nmol/l) was added to six-well plates. HTR-8/SVneo cells were incubated with MitoTracker Green for 30 min at 37°C. Then, the solution was washed away and replaced with fresh RPMI-1640 medium. Cells were observed under a fluorescence microscope (Olympus).

Statistical Analyses

The normal distribution was analyzed with Shapiro-Wilk test. The data were expressed as mean ± standard deviation. The analysis between the two groups was evaluated using the independent samples *t*-test. For the analysis of three or more than three groups, a one-way analysis of variance with a post-hoc comparison using Tukey's method was performed. SPSS 20.0 (IBM, Armonk, NY, USA) was employed for statistical analyses and $P<0.05$ was considered significant.

Results

Ferroptosis Occurs in the VT of TP Patients

Ferroptosis is characterized by iron-dependent accumulation of lipid peroxidation to a lethal level.[19] First, the iron distribution in VT was examined. Staining revealed iron deposits (blue granules) in the cytoplasm of iron-positive cells (Figure 1A). GSH content and GPx activity were decreased, whereas the MDA level was increased, in the VT of TP patients compared with the VT of women who had a normal pregnancy (Figure 1B–D).

To measure protein expression of ferroptosis-related genes, we conducted Western blotting and immunohistochemistry on VT. Western blotting showed that protein expression of SLC7A11 and GPx4 was reduced in the VT of women in the TP group, whereas protein expression of TfR1 and ACSL4 was increased (Figure 1E). Immunohistochemistry (Figure 1F) revealed downregulated expression of SLC7A11 and GPx4 and upregulated expression of TfR1 and ACSL4 in the VT of TP patients. We undertook immunofluorescence staining of GPx4 and TfR1, along with cytokeratin-7 (CK7, a classical cytotrophoblasts marker of VT). Co-immunostaining (Figure 1G) confirmed that GPx4 and TfR1 were expressed mainly in villous trophoblasts instead of in the interstitial layer. This finding suggested that ferroptosis-related genes played a vital part in villus function because the ability of nutrient transport, cell invasion and cell migration in the fetus is initiated mainly by the trophoblast layer. The molecular mechanisms of ferroptosis are dependent upon the production and elimination of lipid peroxidation. Iron and PUFAs "fuel" ferroptosis because they are the raw materials of lipid peroxidation, whereas SLC7A11 and GPx4 regulate ferroptosis. Reduced expression of SLC7A11 and GPx4 and increased expression of TfR1 and ACSL4 in TP patients implied that ferroptosis could be involved in TP pathogenesis.

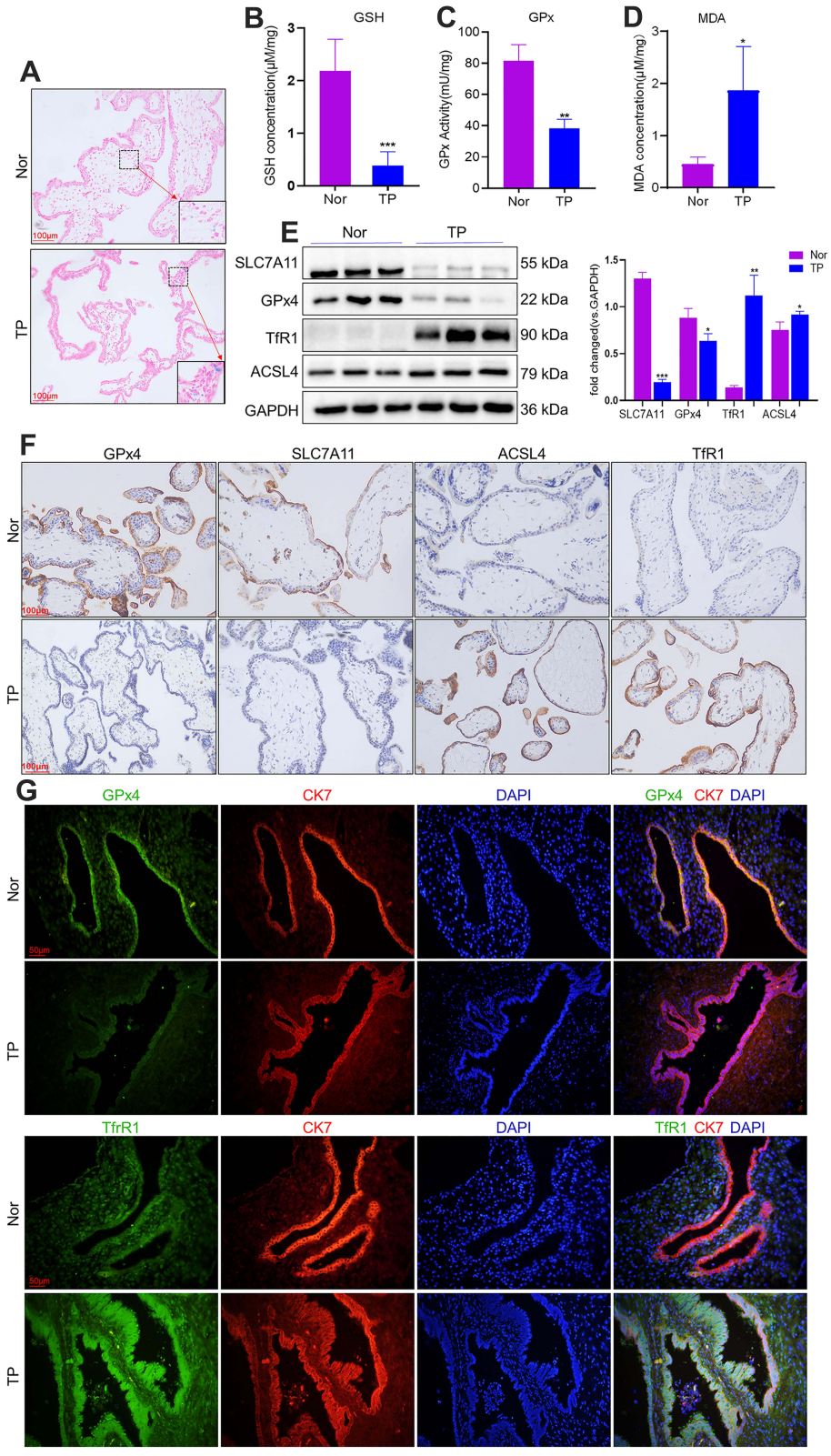

Figure 1 Ferroptosis occurs in the VT of TP patients. VT was collected from patients with TP (n = 15) as well as from women with a normal pregnancy (n = 15). (**A**) Representative images of VT sections with Prussian Blue staining. (**B–D**) GSH content, GPx activity and MDA level were measured using the corresponding detection kits. Expression of proteins closely associated with ferroptosis was measured using Western blotting (**E**) and immunohistochemical staining (**F**). (**G**) Co- immunostaining of the proteins of GPx4, TfR1 with CK7. Nor: control (pregnancy). **P*<0.05, ***P*<0.01, ****P*<0.001 versus Nor group.
Abbreviation: TP, tubal pregnancy.

Exposure to Erastin and RLS3 Triggered Ferroptosis in Trophoblasts

The ferroptosis-induced agents RSL3 and erastin inhibit the expression of GPx4 and Xc^- (cystine/glutamate antiporter system), respectively.[20] The viability of HTR-8/SVneo cells was measured after treatment with erastin (0–4 μM) or RSL3 (0–200 nM), respectively. Erastin and RSL3 induced cell death in a time- and dose-dependent manner (Figure 2A and D). Subsequently, ferroptosis-related features were analyzed upon administration of erastin or RSL3 to investigate if ferroptosis in HTR-8/SVneo cells was induced. Fewer cells and morphologic abnormalities were observed after treatment with erastin (2.5 μM) or RSL3 (0.1 μM) (Figure 2G). Then, the total level of ROS was measured using the DCFH-DA fluorescent probe: the total level of ROS was increased after addition of erastin or RSL3 (p<0.001) for 24 h (Figure 2G).

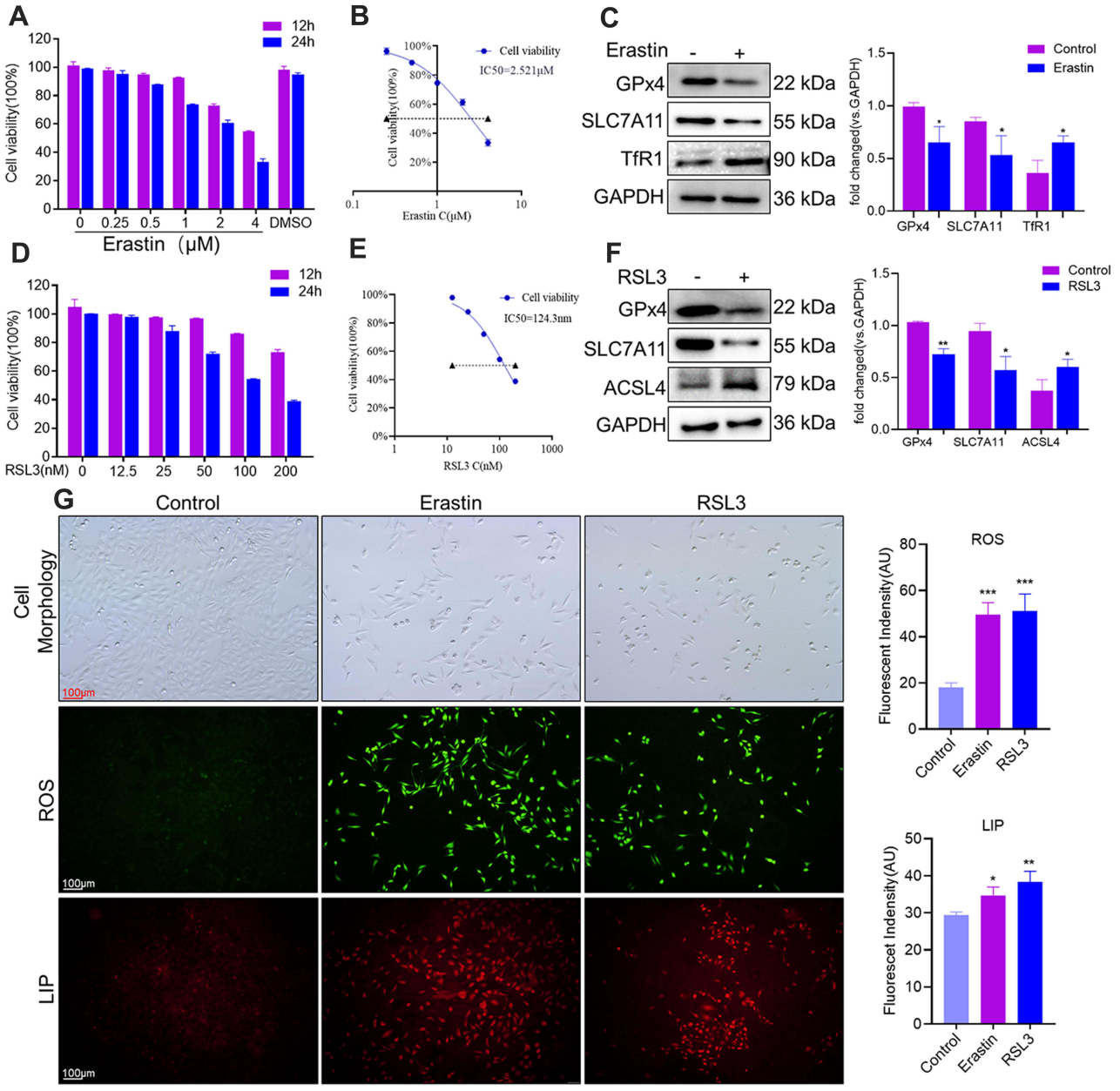

Figure 2 Exposure to erastin and RLS3 triggered ferroptosis in trophoblasts. (**A** and **D**) Ferroptosis was induced in HTR-8/SVneo cells by erastin or RSL3 for 12 h or 24 h, respectively. (**B** and **E**) Half-maximal inhibitory concentration (IC_{50}) of HTR-8/SVneo cells treated with erastin or RSL3 for 24 h. (**C** and **F**) Western blotting of ferroptosis-related proteins induced by erastin or RSL3 for 24 h. *P<0.05, **P<0.01 versus control group. (**G**) Cell morphology, ROS level and LIP content after treatment with erastin or RSL3 for 24 h. Cellular levels of ROS and LIP were measured by a DCFH-DA probe and FeRhoNox-1 probe, respectively. Scale bar = 100 μm. *P<0.05, **P<0.01, ***P<0.001 versus control group.

The mean fluorescence intensity of FeRhoNox-1 (which served as an indirect measure of labile Fe^{2+}) was increased in erastin and RSL3 groups (Figure 2G).

Protein expression of SLC7A11 and GPx4 was lower after exposure to erastin or RSL3. Protein expression of TfR1 and ACSL4 was reduced in erastin and RSL3 groups, respectively (Figure 2C and F). Besides, RSL3 (half-maximal inhibitory concentration (IC_{50}) = 124.3 nM) (Figure 2E) predisposed HTR-8/SVneo cells to ferroptosis compared with erastin (IC_{50} = 2.521 μM) (Figure 2B), so RSL3 was used for subsequent experiments.

Shikonin and RSL3 Inhibited the Viability, Migration and Invasion of Trophoblasts

Ferroptosis-related genes show abundant expression in the decidual cells and trophoblasts of first-trimester placentas.[6] Hence, we investigated whether ferroptosis was involved in the proliferation and migratory capacity of trophoblasts. The Cell Counting Kit (CCK) 8 assay showed that shikonin enhanced the inhibition of RSL3 (0.1 μM) on cell viability in a time- and concentration-dependent manner (Figure 3A). In addition, Fer-1 (a small-molecule inhibitor of lipid peroxidation) and deferoxamine (iron chelator) blocked the cell death induced by shikonin (1.2 μM) alone or in concert with RSL3 (0.1 μM) (Figure 3B). Subsequently, assays were conducted to examine the invasive and migratory abilities of trophoblasts. The number of invading cells was decreased and wound closure was delayed

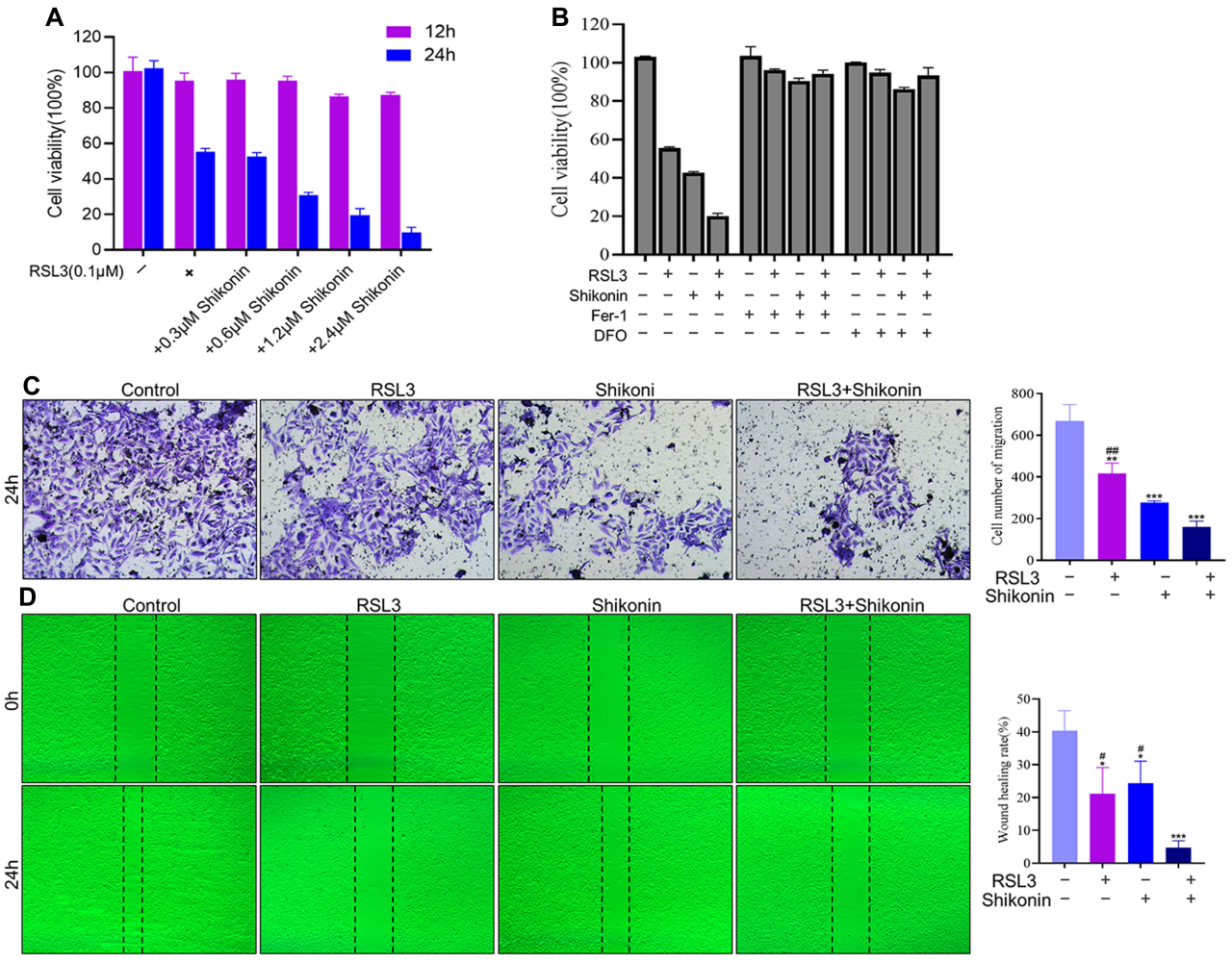

Figure 3 Shikonin and RSL3 inhibited the viability, migration and invasion of trophoblasts. (**A**) Effects of different concentrations and duration of treatment of shikonin on RSL3-induced cell death. (**B**) Treatment with Fer-1 or deferoxamine was undertaken for 4 h before treatment with RSL3 (0.1 μM) alone or in combination with shikonin (1.2 μM) for 24 h, and cell viability was analyzed. (**C** and **D**) HTR-8/SVneo cells were treated with RSL3 (0.1 μM) alone or in combination with shikonin (0.6 μM) for 24 h. The migration and invasion of cells were detected by Transwell™ and wound-healing assays, respectively. Corresponding quantitative histograms are shown on the right. **P*<0.05, ***P*<0.01, ****P*<0.001 versus control group; #*P*<0.05, ##*P*<0.01 versus RSL3+shikonin group.

after exposure to shikonin alone or in combination with RSL3 compared with that in the negative-control group (Figure 3C and D). These results indicated that ferroptosis could be a target to cure TP by inhibition of the viability, migration and invasion of trophoblasts, and that a combination of shikonin and ferroptosis amplified this suppression.

Shikonin Sensitized HTR-8/SVneo Cells to Ferroptosis, Accompanied by ROS Production and Lipid Peroxidation

Given that inhibition of GPx4 expression facilitated ROS accumulation as well as the relationship between shikonin and ROS, this research investigated whether cotreatment of shikonin with RSL3 could alter the ROS level. Shikonin used alone or in combination with RSL3 restrained the GPx activity (Figure 4A), GSH concentration (Figure 4B) and enhanced MDA activity (Figure 4C) dramatically in HTR-8/SVneo cells. Hence, shikonin used alone or in combination with RSL3 could drive ROS production in trophoblasts. Then, we measured lipid peroxidation by staining viable cells with the lipid-ROS probe C11-BODIPY: cotreatment of shikonin with RSL3 promoted lipid peroxidation markedly compared with that obtained through treatment with either agent alone (Figure 4D).

We evaluated if shikonin influenced protein expression of GSH, SLC7A11, ACSL4 and TfR1. The use of RSL3 alone or shikonin alone increased protein expression of GPx4 and SLC7A11 and inhibited protein expression of ACSL4 in trophoblasts, and could be amplified by the cotreatment of RSL3 and shikonin (Figure 4E). However, a change in TfR1 expression was not observed under either RSL3 or shikonin exposure. The IF staining of GPx4 and ACSL4 in HTR-8/SVneo cells revealed results consistent with data from Western blotting, and GPx4 and ACSL4 were expressed in the cytoplasm and plasma membrane, respectively (Figure 4F). These results suggested that shikonin alone or in the presence of RSL3 inhibited GSH synthesis and led to excessive production of ROS, which gave rise to failure of antioxidant mechanisms.

Shikonin Sensitized HTR-8/SVneo Cells to Ferroptosis in an Autophagy-Independent Manner

Previously, we demonstrated that shikonin promotes autophagy in HTR-8/SVneo cells.[21] Thus, this study investigated whether shikonin sensitizes cells to ferroptosis via autophagy. Western blotting showed that the combination of RSL3 and shikonin did not alter the protein expression of LC3B or P62 (Figure 5A). Labile Fe^{2+} is vital for ferroptosis because it contributes greatly to the generation of lipid peroxides. Levels of LIP and ROS in HTR-8/SVneo cells, which were increased under exposure to RLS3 and shikonin could be restrained by Fer-1, but not by chloroquine (Figure 5B). Similarly, the downregulation of expression of GPx4 and SLC7A11 and upregulation of ACSL4 expression after cotreatment with RSL3 and shikonin could be reversed by Fer-1, but a response to chloroquine was not elicited (Figure 5C). These results demonstrated that the cell death induced by a combination of RSL3 and shikonin was ferroptosis and was independent of autophagy.

Activation of Nrf2 Alleviated Sensitization of Shikonin to Ferroptosis

Considering that shikonin had no effect on TfR1 expression and was related mainly to lipid peroxidation, this research further analyzed the structure of shikonin. The structure of shikonin was mapped by ChemDraw software 20.0 (Supplementary Figure S1A), and we predicted potential targets for shikonin via Bioinformatics Analysis Tool for Molecular Mechanism of Traditional Chinese Medicine (BATMAN-TCM13; http://bionet.ncpsb.org/batman-tcm/) and found a key gene: NQO1 (Supplementary Figure S1B). Then, the protein–protein interactions (PPIs) of NQO1 and ferroptosis were predicted in the Search Tool for the Retrieval of Interacting Genes/Proteins (STRING) database (https://string-db.org/) (Supplementary Figure S1C). NQO1 expression is regulated by Nrf2 and studies have shown that shikonin promotes ROS production by inhibiting Nrf2 expression.[16,22] Hence, this experiment investigated the role of Nrf2 during ferroptosis induced by simultaneous exposure to shikonin and RSL3.

Nrf2 is located mainly in the cytoplasm under physiological conditions. However, in response to oxidative stress, Nrf2 translocates to the nucleus to initiate the transcription of cytoprotective genes.[23] The IF experiment was conducted to observe the effect of RSL3, shikonin and their combination on Nrf2 expression in a hypoxic environment (Figure 6A). Nrf2 is mostly located in the nuclear of control cells, and less located in the nuclear

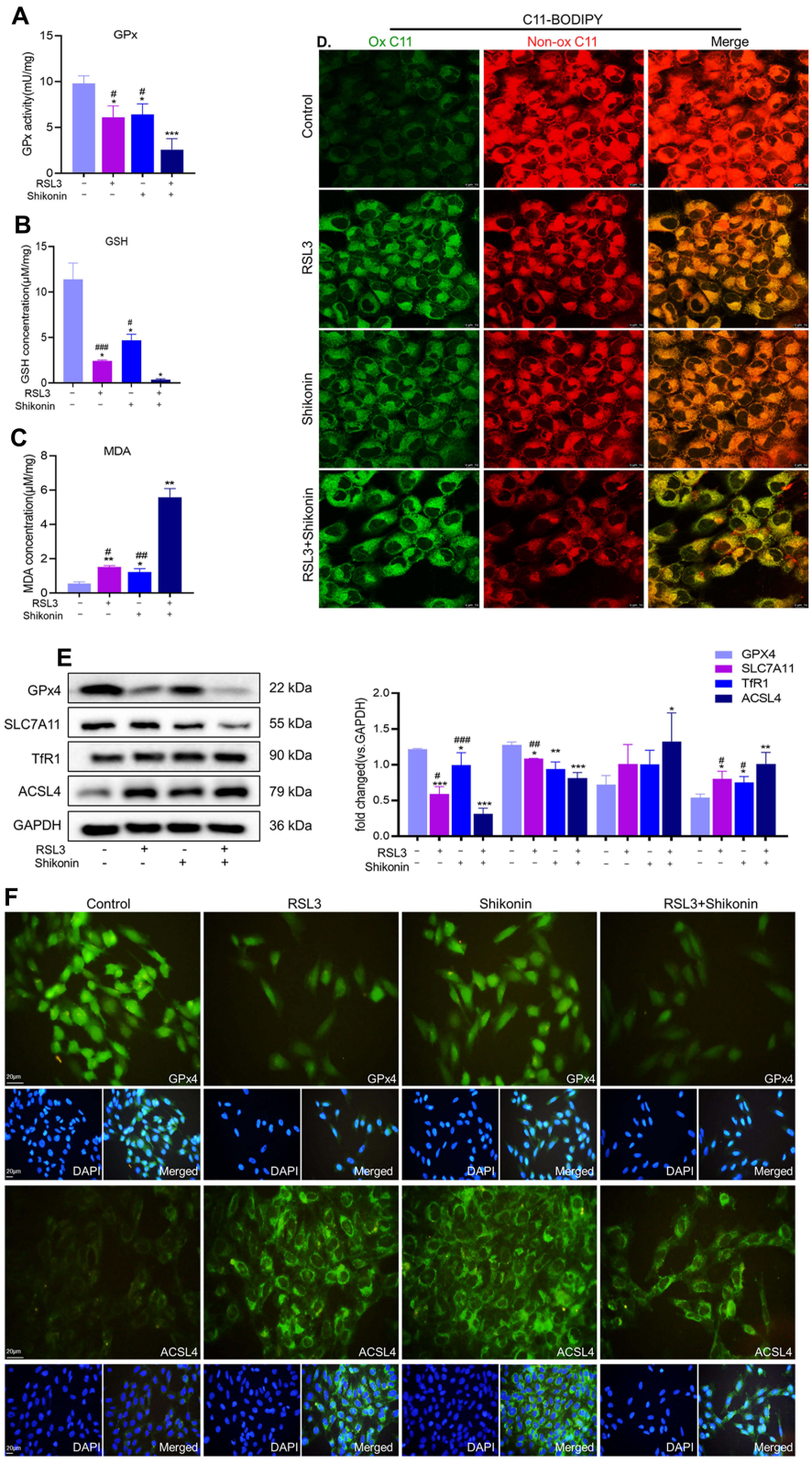

Figure 4 Shikonin sensitized HTR-8/SVneo cells to ferroptosis. HTR-8/SVneo cells were treated with shikonin (0.6 μM) alone or in combination with RSL3 (0.1 μM) for 24 h. (**A**–**C**). GSH content, GPx activity and MDA level were measured using the corresponding detection kits. *P<0.05, **P<0.01, ***P<0.001 versus control group; $^{\#}P$<0.05, $^{\#\#}P$<0.01, $^{\#\#\#}P$<0.001 versus RSL3+shikonin group. (**D**) Lipid peroxidation in HTR-8/SVneo cells was visualized through the C11-BODIPY™ probe and observed by confocal laser scanning microscopy. Scale bar = 10 μm. (**E**) Western blotting measured protein expression of GPx4, SLC7A11, ACSL4 and TfR1 in HTR-8/SVneo cells. Corresponding quantitative histograms are shown on the right. *P<0.05, **P<0.01, ***P<0.001 versus control group; $^{\#}P$<0.05, $^{\#\#}P$<0.01, $^{\#\#\#}P$<0.001 versus RSL3+shikonin group. (**F**) Protein expression of GPx4 and ACSL4 according to immunofluorescence staining.

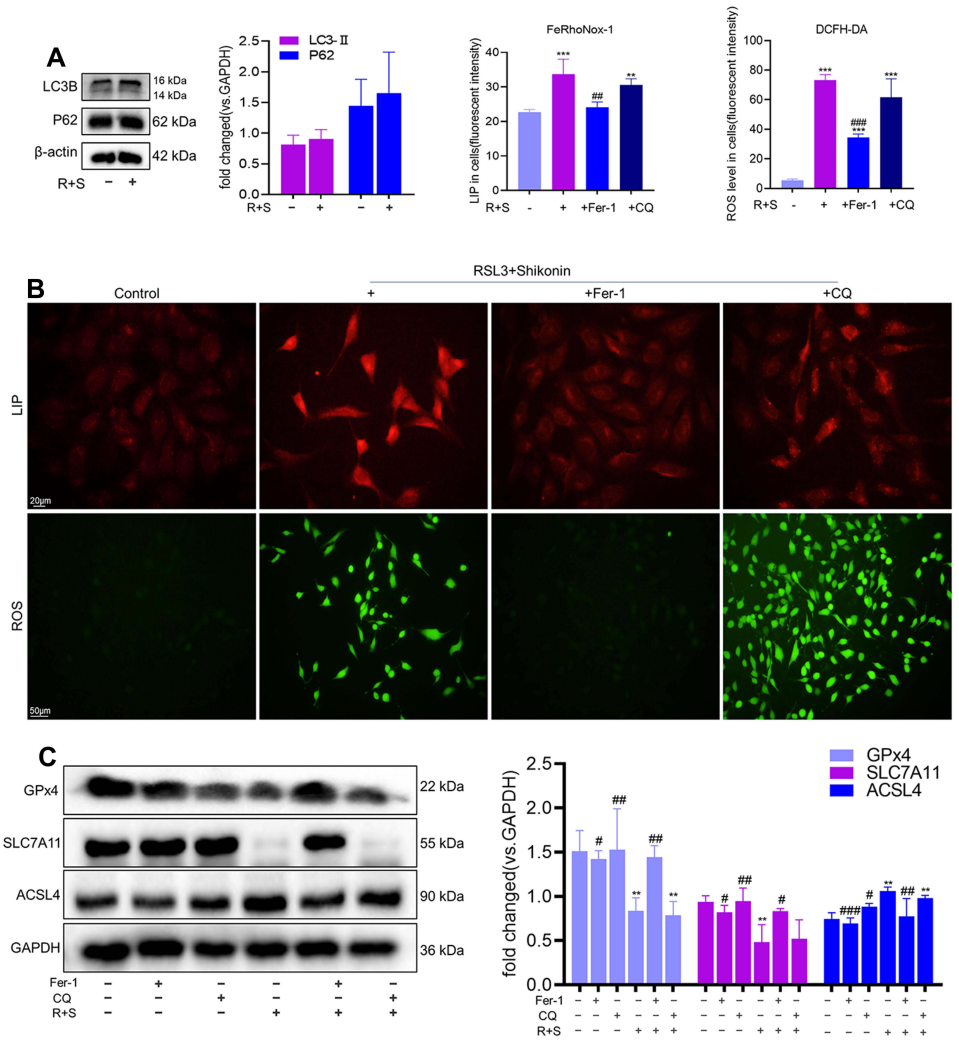

Figure 5 Shikonin sensitized HTR-8/SVneo cells to ferroptosis in an autophagy-independent manner. (**A**) Western blotting detected protein expression of LC3B and P62 in HTR-8/SVneo cells after cotreatment of RSL3 (0.1 μM) with shikonin (0.6 μM). (**B**) Cellular levels of LIP and ROS in HTR-8/SVneo cells after treatment with RSL3+shikonin in the presence or absence of the indicated inhibitors were determined by the DCFH-DA probe and FeRhoNox-1 probe, respectively. Pretreatment with Fer-1 or chloroquine was undertaken for 4 h. Corresponding quantitative histograms are shown on the upper right. $^{**}P<0.01$, $^{***}P<0.001$ versus control group; $^{\#\#}P<0.01$, $^{\#\#\#\#}P<0.001$ versus RSL3+shikonin group. LIP: scale bar = 20 μm, ROS: scale bar = 50 μm. (**C**) Western blotting detected protein expression of GPx4, SLC7A11, ACSL4 in HTR-8/SVneo cells treated with RSL3+shikonin in the presence or absence of the indicated inhibitors. Pretreatment with Fer-1 or chloroquine was undertaken for 4 h. Corresponding quantitative histograms are shown on the right. $^{**}P<0.01$ versus control group; $^{\#}P<0.05$, $^{\#\#}P<0.01$, $^{\#\#\#\#}P<0.001$ versus RSL3+shikonin group.

under treatment with RSL3 or shikonin alone, and predominantly located in cytoplasm under the combination of use of RSL3 and shikonin, which suggests that RSL3 or/and shikonin inhibited Nrf2 activation markedly. Next, Nrf2 was activated pharmacologically by t-BHQ pretreatment. Pretreatment with t-BHQ (20 μM or 40 μM) for 6 h rescued cell death dramatically before the co-treatment of RSL3 with shikonin (Figure 6B). Hence, t-BHQ at 20 μM was selected for subsequent experiments.

Mitochondrial morphology is an intuitive feature of mitochondrial function. First, the mitochondria was labeled via MitoTracker Green. An elongated-mitochondrial network appeared in the control group and in the presence of t-BHQ. Upon exposure to shikonin + RSL3, the mitochondria of HTR-8/SVneo cells became fragmented and accumulated around nuclei (Figure 6B). This result revealed that shikon + RSL3 induced an imbalance of mitochondrial dynamics that could be restored by Nrf2. Besides, a high ROS level produced by shikonin + RSL3 treatment was reversed by supplementation with t-BHQ (Figure 6B). Western blotting (Figure 6C) revealed that shikonin + RSL3 therapy reduced expression of Nrf2 and NQO1, which could be reversed by use of the Nrf2 inducer t-BHQ. These results suggested that cotreatment of shikonin with RSL3 repressed Nrf2 activation and expression of its downstream transcription factor

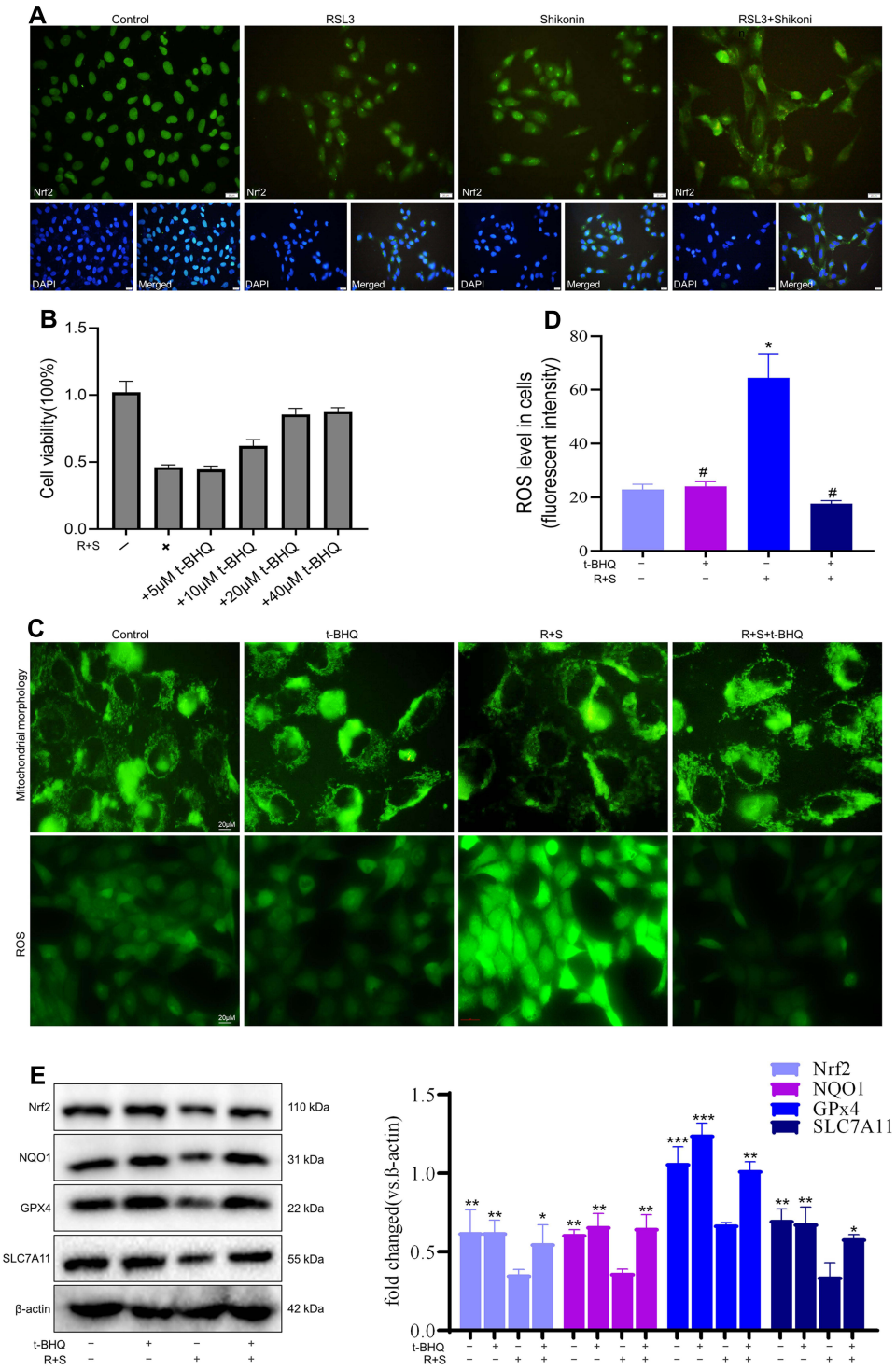

Figure 6 Supplementation with Nrf2 alleviated sensitization of shikonin to ferroptosis. Cells were treated with t-BHQ for 6 h before treatment with RSL3 (0.1 μM) + shikonin (0.6 μM). (**A**) Representative immunofluorescence images show Nrf2 transferred from the cytoplasm to the nucleus after treatment with RSL3 alone or in combination with shikonin. (**B**) Cell viability. (**C**) Representative images of mitochondrial morphology and cellular ROS level. HTR-8/SVneo cells were treated with RSL3 +shikonin for 24 h after pretreatment with t-BHQ for 6 h. Scale bar = 20 μm. Corresponding quantitative histograms are shown as (**D**). **P*<0.05, versus control group; #*P*<0.05 versus RSL3+shikonin group. (**E**) Western blotting detected Nrf2 expression and downstream protein expression in HTR-8/SVneo cells. **P*<0.05, ***P*<0.01, ****P*<0.001 versus RSL3+shikonin group.

NQO1, whereas the Nrf2 inducer increased expression of NQO1, SLC7A11 and GPx4. These data implied that the promoting effect of shikonin on lipid peroxidation was caused mainly by inhibition of Nrf2 expression.

We further verified the connection between Nrf2 and TP. Higher expression of Nrf2 protein was observed in the Nor (control (pregnancy)) group compared with that in the TP group (Supplementary Figure S2A). IHC (Supplementary Figure S2B) and IF (Supplementary Figure S2C) images demonstrated that the brown granules and mean fluorescence intensity of Nrf2 were significantly stronger in the Nor group, and were distributed mainly in cytoplasm. Nrf2 plays an important role in the maintenance of cellular redox by regulating detoxification, antioxidants and NADPH-regeneration enzymes. Low expression of Nrf2 failed to regulate the imbalance of oxidative stress induced by a pathologic pregnancy, which could be an important factor in the occurrence and progression of TP.

Discussion

Early embryonic development requires a hypoxic environment. However, the hypoxic environment is more obvious in TP because the fallopian tubes fail to build a complete decidua. Oxidative stress has been implicated in TP pathogenesis, and ferroptosis is driven by lipid peroxidation, a consequence of cellular metabolism and imbalanced redox homeostasis. There is insufficient evidence to suggest that ferroptosis occurs in TP.

The manner in which cystine is introduced into GSH-GPx4 was the first pathway of ferroptosis to be discovered.[24] SLC7A11 is a key component of the Xc^- system, which mediates uptake of extracellular cystine in exchange for intracellular glutamate, and then cystine is converted rapidly to cysteine as the raw material for intracellular GSH synthesis.[25] GSH detoxifies lipid hydroperoxides to lipid alcohols through the enzyme activity of GPx to limit the spread of lipid peroxidation in the membrane. If GPx4 is dysfunctional, then phospholipid hydroperoxides can trigger a catalytic reaction in the presence of excess iron, resulting in ferroptosis. GSH, GPx and MDA are important indices to evaluate the degree of lipid peroxidation, so they can help determine if ferroptosis occurs in TP. In the present study, reduced GSH content and GPx activity and increased MDA level in TP indicated changes in the balance of the oxidant–antioxidant system, which impaired mitochondrial activity and ciliary motility in the tubal epithelium.[3]

Iron in the blood circulation is composed mainly of ferric ions (Fe^{3+}). It is transported into cells through TfR1 and endocytosis to form endosomes.[26] Western blotting and IHC revealed that TfR1 (the principal protein responsible for the cellular uptake of iron) expression was increased significantly in TP. Similarly, staining (Prussian Blue) showed deposition of iron particles to be more obvious in the TP group. These data implied that the iron element required for lipid peroxidation was abundant in TP and iron overload might be one of the risk factors of TP Previous study revealed that excessive iron intake or high iron status might be related to reproductive diseases, such as endometriosis and preeclampsia.[27] Hence, attention should be paid to the fine regulation of iron level during pregnancy.

Screening of human haploid cells has revealed that ACSL4 fuels ferroptosis because it preferentially activates long PUFAs for phospholipid biosynthesis.[28] Subsequently, ACSL4 was considered to be a hallmark of ferroptosis sensitivity because it "shapes" the lipid composition in cells.[28–30] We discovered that ACSL4 expression was increased in TP patients and promoted PUFA synthesis. This research revealed, for the first time, that a hypoxic microenvironment, abundant iron element, and PUFA-LA substrates contribute together to aid ferroptosis in TP.

The main pathology of TP lies in the proliferation and invasion of extra-villous trophoblasts, which can lead to local hemorrhage and rupture.[31] Accordingly, inhibition of the invasion and migration of trophoblasts has been explored as a drug treatment for TP. Studies have shown that erastin exposure attenuates the proliferation and migration abilities of endothelial cells.[32] The migration and invasion ability of clear cell renal cell carcinoma cells can be inhibited by Kruppel-like factor 2-mediated GPx4 transcription through regulation of ferroptosis.[33] Herein, ferroptosis of HTR-8/SVneo cells could be induced under application of RSL3 or erastin, and they were more sensitive to RSL3 stimulation. This study discovered that RSL3 inhibited proliferation, invasion and migration of HTR-8/SVneo, which helped to determine that targeting ferroptosis in trophoblasts could be a promising treatment of TP. Besides, on the one hand, shikonin could further inhibit cell proliferation induced by RSL3 to help to eliminate the TP tissue; on the other hand, shikonin could inhibit cell invasion and migration abilities induced by RSL3 to prevent rupture and bleeding in the TP tissue. These data made us aware of the potential of shikonin as a treatment for TP. At present, methotrexate (MTX) is a prevalent drug to treat TP via inhibiting DNA synthesis in actively dividing trophoblasts,[31] but MTX is also

a chemotherapeutic agent that can have adverse consequences, including gastrointestinal symptoms, hepatic enzyme abnormalities and bone marrow suppression.[34] Natural products have the characteristics of high chemical diversity and biochemical specificity. As a natural product, shikonin is an attractive clinical candidate compound in the quest for new TP treatments. Compared to MTX, shikonin comes from a wider range of sources, and displays favorable absorption, distribution, metabolism, excretion, and toxicity characteristics.[35]

In view of the ROS-promoting properties of shikonin and its ability to inhibit invasion and migration, it was necessary to further explore whether shikonin enhanced ferroptosis in HTR-8/SVneo cells. First, this research demonstrated that shikonin reduced GPx activity and GSH content, increased the MDA level and promoted production of ROS. These data are consistent with studies showing that shikonin triggers GSH depletion and further induces accumulation of ROS.[36,37] Besides, shikonin inhibited the expression of GPx4 and SLC7A11 and increased the expression of ACSL4, but had no effect on TfR1 expression. Hence, we believe that shikonin mainly affects GSH synthesis and enhances intracellular ROS accumulation, thereby amplifying lipid peroxidation and promoting the sensitivity to iron-based death, rather than affecting iron intake. Furthermore, we previously demonstrated that shikonin stimulated autophagy.[21] Autophagy has been reported to promote ferroptosis by degrading ferritin, thereby increasing cellular labile-iron content.[38] However, these results indicated that shikonin sensitized ferroptosis in an autophagy-independent manner.

Considering that shikonin had no effect on iron transporters and was not dependent upon autophagy, this study explored the mechanism by which shikonin promotes sensitivity to iron-based death from the perspective of lipid ROS. As a quinone-containing natural product, shikonin has been reported to increase ROS generation and inhibit nuclear Nrf2 expression in glioma cells.[16] As a stress-inducible transcription factor, Nrf2 is a "master regulator" of the antioxidant response, and has been reported to regulate the activity of several ferroptosis-related proteins: SLC7A11, GPx4 and FTH1.[15] Furthermore, Nrf2 expression has been correlated directly with ferroptosis sensitivity. Increased expression of Nrf2 prevents ferroptosis,[39] whereas inhibition of the Nrf2-ARE pathway increases the sensitivity of cancer cells to pro-ferroptotic agents.[40] Herein, RSL3, shikonin and their combination inhibited nuclear accumulation of Nrf2, and reduced protein expression of the Nrf2-cascade genes NQO1, SLC7A11 and GPx4, which suggested that RSL3 alone or in combination with shikonin inhibited Nrf2 signaling to accelerate oxidative stress. Hence, the ROS generated by shikonin inhibited nuclear translocation of Nrf2, which further inhibited the antioxidant ability of Nrf2 and, finally, magnified ferroptosis.

The greater staining intensity of MitoTracker Green in the shikonin + RSL3 group suggested that mitochondrial dysfunction could lead to oxidative phosphorylation in mitochondria. Therefore, the results suggest that the excessive production of ROS caused by cotreatment of shikonin with RSL3 may be due (at least in part) to the destruction of mitochondrial structure, except for lipid oxidation by Fe^{2+}. Furthermore, the activation of Nrf2 rescued cellular ROS and ROS produced by mitochondrial damage under shikonin + RSL3 exposure. Subsequent verification of significant expression of Nrf2 protein in the VT of TP patients also implied the clinical potential of shikonin through regulation of Nrf2 expression to promote ferroptosis in TP treatment.

The availability of fallopian tubes from healthy pregnant women and women suffering from TP for comparison is limited due to ethical reasons. Also, an animal model of TP is lacking. Hence, these investigations were performed on VT and HTR-8/SVneo cells.

Conclusion

This research firstly revealed that (i) ferroptosis may be an underlying mechanism affecting the occurrence and development of TP; (ii) shikonin sensitized cells to ferroptosis through a Nrf2 signaling cascade. This study could provide a new perspective for the clinical drug development of TP.

Acknowledgements

We thank Ms. Shuo Yuan for technical assitance and the Sport-University-Klarity Joint Laboratory for technical support.

Author Contributions

All authors contributed to data analysis, drafting or revising the article, have agreed on the journal to which the article was submitted, gave final approval for the version to be published, and agreed to be accountable for all aspects of the work.

Funding

This work was supported by the National Natural Science Foundation of China (82174417; 81804134); the Natural Science Foundation of Guangdong Province (2018A030313469); the Department of Education of Guangdong Province (2021ZDZX2036; 2019GCZX009); and first-class discipline research key project of Guangzhou University of Chinese Medicine (2020, No. 6).

Disclosure

The authors report no conflicts of interest in this work.

References

1. Brady PC. New evidence to guide ectopic pregnancy diagnosis and management. *Obstet Gynecol Surv*. 2017;72(10):618–625. doi:10.1097/OGX.0000000000000492
2. Bianchi E, Sun Y, Almansa-Ordonez A, et al. Control of oviductal fluid flow by the G-protein coupled receptor Adgrd1 is essential for murine embryo transit. *Nat Commun*. 2021;12(1):1251. doi:10.1038/s41467-021-21512-w
3. Tok A, Özer A, Baylan FA, Kurutaş EB. Copper/Zinc ratio can be a marker to diagnose ectopic pregnancy and is associated with the oxidative stress status of ectopic pregnancy cases. *Biol Trace Elem Res*. 2021;199(6):2096–2103. doi:10.1007/s12011-020-02327-0
4. Beharier O, Kajiwara K, Sadovsky Y. Ferroptosis, trophoblast lipotoxic damage, and adverse pregnancy outcome. *Placenta*. 2021;108:32–38. doi:10.1016/j.placenta.2021.03.007
5. Jiang X, Stockwell BR, Conrad M. Ferroptosis: mechanisms, biology and role in disease. *Nat Rev Mol Cell Biol*. 2021;22(4):266–282. doi:10.1038/s41580-020-00324-8
6. Ng SW, Norwitz SG, Norwitz ER. The impact of iron overload and ferroptosis on reproductive disorders in humans: implications for preeclampsia. *Int J Mol Sci*. 2019;20(13):3283. doi:10.3390/ijms20133283
7. Cao Y, Traer E, Zimmerman GA, McIntyre TM, Prescott SM. Cloning, expression, and chromosomal localization of human long-chain fatty acid-CoA ligase 4 (FACL4). *Genomics*. 1998;49(2):327–330. doi:10.1006/geno.1998.5268
8. Cao Y, Murphy KJ, McIntyre TM, Zimmerman GA, Prescott SM. Expression of fatty acid-CoA ligase 4 during development and in brain. *FEBS Lett*. 2000;467(2–3):263–267. doi:10.1016/S0014-5793(00)01159-5
9. Uhlén M, Fagerberg L, Hallström BM, et al. Proteomics. Tissue-based map of the human proteome. *Science*. 2015;347(6220):1260419.
10. Chen CH, Lin ML, Ong PL, Yang JT. Novel multiple apoptotic mechanism of shikonin in human glioma cells. *Ann Surg Oncol*. 2012;19(9):3097–3106. doi:10.1245/s10434-012-2324-4
11. Gupta P, Jagavelu K, Mishra DP. Inhibition of NADPH oxidase-4 potentiates 2-deoxy-D-glucose-induced suppression of glycolysis, migration, and invasion in glioblastoma cells: role of the Akt/HIF1α/HK-2 signaling axis. *Antioxid Redox Signal*. 2015;23(8):665–681. doi:10.1089/ars.2014.5973
12. Duan D, Zhang B, Yao J, Liu Y, Fang J. Shikonin targets cytosolic thioredoxin reductase to induce ROS-mediated apoptosis in human promyelocytic leukemia HL-60 cells. *Free Radic Biol Med*. 2014;70:182–193. doi:10.1016/j.freeradbiomed.2014.02.016
13. Oh ET, Park HJ. Implications of NQO1 in cancer therapy. *Bmb Rep*. 2015;48(11):609–617. doi:10.5483/BMBRep.2015.48.11.190
14. Ray PD, Huang BW, Tsuji Y. Reactive oxygen species (ROS) homeostasis and redox regulation in cellular signaling. *Cell Signal*. 2012;24(5):981–990. doi:10.1016/j.cellsig.2012.01.008
15. Dodson M, Castro-Portuguez R, Zhang DD. NRF2 plays a critical role in mitigating lipid peroxidation and ferroptosis. *Redox Biol*. 2019;23:101107. doi:10.1016/j.redox.2019.101107
16. Yang JT, Li ZL, Wu JY, Lu FJ, Chen CH. An oxidative stress mechanism of shikonin in human glioma cells. *PLoS One*. 2014;9(4):e94180. doi:10.1371/journal.pone.0094180
17. Graham CH, Hawley TS, Hawley RG, et al. Establishment and characterization of first trimester human trophoblast cells with extended lifespan. *Exp Cell Res*. 1993;206(2):204–211. doi:10.1006/excr.1993.1139
18. Abou-Kheir W, Barrak J, Hadadeh O, Daoud G. HTR-8/SVneo cell line contains a mixed population of cells. *Placenta*. 2017;50:1–7. doi:10.1016/j.placenta.2016.12.007
19. Friedmann AJ, Krysko DV, Conrad M. Ferroptosis at the crossroads of cancer-acquired drug resistance and immune evasion. *Nat Rev Cancer*. 2019;19(7):405–414. doi:10.1038/s41568-019-0149-1
20. Stockwell BR, Friedmann AJ, Bayir H, et al. Ferroptosis: a regulated cell death nexus linking metabolism, redox biology, and disease. *Cell*. 2017;171(2):273–285. doi:10.1016/j.cell.2017.09.021
21. Wang Y, Zhu F, Zhang Y, et al. Shikonin suppresses trophoblast cell growth via regulation of GLI1, and p62 mediated caspase 8 activation. *Reprod Toxicol*. 2020;95:104–112. doi:10.1016/j.reprotox.2020.05.011
22. Ko H, Kim SJ, Shim SH, Chang H, Ha CH. Shikonin Induces apoptotic cell death via regulation of p53 and Nrf2 in AGS human stomach carcinoma cells. *Biomol Ther*. 2016;24(5):501–509. doi:10.4062/biomolther.2016.008
23. Sandberg M, Patil J, D'Angelo B, Weber SG, Mallard C. NRF2-regulation in brain health and disease: implication of cerebral inflammation. *Neuropharmacology*. 2014;79:298–306. doi:10.1016/j.neuropharm.2013.11.004
24. Dixon SJ, Lemberg KM, Lamprecht MR, et al. Ferroptosis: an iron-dependent form of nonapoptotic cell death. *Cell*. 2012;149(5):1060–1072. doi:10.1016/j.cell.2012.03.042
25. Koppula P, Zhang Y, Zhuang L, Gan B. Amino acid transporter SLC7A11/xCT at the crossroads of regulating redox homeostasis and nutrient dependency of cancer. *Cancer Commun*. 2018;38(1):12. doi:10.1186/s40880-018-0288-x
26. Brown R, Richardson KL, Kabir TD, Trinder D, Ganss R, Leedman PJ. Altered iron metabolism and impact in cancer biology, metastasis, and immunology. *Front Oncol*. 2020;10:476. doi:10.3389/fonc.2020.00476
27. Dewey KG, Oaks BM. U-shaped curve for risk associated with maternal hemoglobin, iron status, or iron supplementation. *Am J Clin Nutr*. 2017;106(Suppl 6):1694S–1702S. doi:10.3945/ajcn.117.156075

28. Dixon SJ, Winter GE, Musavi LS, et al. Human haploid cell genetics reveals roles for lipid metabolism genes in nonapoptotic cell death. *Acs Chem Biol*. 2015;10(7):1604–1609. doi:10.1021/acschembio.5b00245
29. Doll S, Proneth B, Tyurina YY, et al. ACSL4 dictates ferroptosis sensitivity by shaping cellular lipid composition. *Nat Chem Biol*. 2017;13 (1):91–98. doi:10.1038/nchembio.2239
30. Drijvers JM, Gillis JE, Muijlwijk T, et al. Pharmacologic screening identifies metabolic vulnerabilities of CD8(+) T cells. *Cancer Immunol Res*. 2021;9(2):184–199. doi:10.1158/2326-6066.CIR-20-0384
31. Murray H, Baakdah H, Bardell T, Tulandi T. Diagnosis and treatment of ectopic pregnancy. *CMAJ*. 2005;173(8):905–912. doi:10.1503/cmaj.050222
32. Lopes-Coelho F, Martins F, Hipólito A, et al. The activation of endothelial cells relies on a ferroptosis-like mechanism: novel perspectives in management of angiogenesis and cancer therapy. *Front Oncol*. 2021;11:656229. doi:10.3389/fonc.2021.656229
33. Lu Y, Qin H, Jiang B, et al. KLF2 inhibits cancer cell migration and invasion by regulating ferroptosis through GPX4 in clear cell renal cell carcinoma. *Cancer Lett*. 2021;522:1–13. doi:10.1016/j.canlet.2021.09.014
34. Auger N, Ayoub A, Wei SQ. Letrozole: future alternative to methotrexate for treatment of ectopic pregnancy? *Fertil Steril*. 2020;114(2):273–274. doi:10.1016/j.fertnstert.2020.04.063
35. Corson TW, Crews CM. Molecular understanding and modern application of traditional medicines: triumphs and trials. *Cell*. 2007;130(5):769–774. doi:10.1016/j.cell.2007.08.021
36. Gao D, Hiromura M, Yasui H, Sakurai H. Direct reaction between shikonin and thiols induces apoptosis in HL60 cells. *Biol Pharm Bull*. 2002;25 (7):827–832. doi:10.1248/bpb.25.827
37. Lu B, Wang Z, Ding Y, et al. RIP1 and RIP3 contribute to shikonin-induced glycolysis suppression in glioma cells via increase of intracellular hydrogen peroxide. *Cancer Lett*. 2018;425:31–42. doi:10.1016/j.canlet.2018.03.046
38. Hou W, Xie Y, Song X, et al. Autophagy promotes ferroptosis by degradation of ferritin. *Autophagy*. 2016;12(8):1425–1428. doi:10.1080/15548627.2016.1187366
39. Fan Z, Wirth AK, Chen D, et al. Nrf2-Keap1 pathway promotes cell proliferation and diminishes ferroptosis. *Oncogenesis*. 2017;6(8):e371. doi:10.1038/oncsis.2017.65
40. Roh JL, Kim EH, Jang H, Shin D. Nrf2 inhibition reverses the resistance of cisplatin-resistant head and neck cancer cells to artesunate-induced ferroptosis. *Redox Biol*. 2017;11:254–262. doi:10.1016/j.redox.2016.12.010